UDK: 378.4:623.463.3:517.962.8
COSATI: 20-12, 19-07

Development of a Closely Coupled Procedure for Dynamic Aeroelastic Analyses

Erkut Başkut[1)]
Ali Akgül[1)]

In this paper, a numerical method is developed to predict the aeroelastic response and the flutter boundary of elastic structures. A closely coupled approach is used for time advancing. The flow solver relies on inviscid Euler equations with finite volume discretization. A modal approach is used for a structural response and the Newmark algorithm is used for time marching. In order to exchange displacement and pressure data between structural and aerodynamic grids, the infinite spline method is used. The Computational Fluid Dynamic mesh is moved based on the spring-based smoothing and the local re-meshing method provided by the FLUENT User Defined Function in order to adapt a new shape of the aerodynamic surface at each aeroelastic iteration. The AGARD Wing 445.6 is modeled and solved with the developed procedure. The obtained results are compared with numerical and experimental data available in the literature.

Key words: **aeroelasticity, dynamic aeroelasticity, wing, flutter, finite element method, algorithm.**

Notation and symbols

b – Half chord length
CFD – Computational Fluid Dynamics
CSD – Computational Structural Dynamics
FSI – Flutter speed Index
Q – Generalized unsteady aerodynamic forces
δ – Displacement
ζ – Damping ratio
V_f – Flutter speed
υ – Mass ratio
ω – Natural frequency

Introduction

AEROELASTIC problems should be considered in the early phase of the air-vehicle structural design since any unstable response to aerodynamic loading may rapidly lead to a disastrous structural failure, which may only be treated by major and usually expensive modifications. Wind-tunnel or flight tests are two expensive methods performed in the late phase of the design. Therefore, computational aeroelasticity methods are used in order to determine aeroelastic characteristics of an air vehicle during its development stages. Dynamic aeroelasticity is concerned with the oscillatory effects of the aerodynamic forces [6]. Flutter is the main area of interest of the dynamic aeroelasticity. Flutter can be defined as an unstable self-excited oscillation in which the structure gains energy from the air stream and leads to a catastrophic structural failure.

Different levels of complexity may be used in order to model the fluid and structure in computational aeroelasticity. In general, as the complexity in physics and geometry increases, so does the accuracy of the obtained results and computational time. The accuracy of aeroelastic modeling can be improved by using high-level aerodynamic models based on the conservation laws and finite element formulation of the structure. These methods fully account for nonlinear effects during aeroelastic analysis, which results in a more accurate prediction of the aeroelastic response and instabilities. Continuity, momentum and energy conservation laws together with the equation of state are generally utilized by CFD methods in order to solve the flow around air vehicles. The Navier-Stokes equations may also be solved for viscous flows. The Euler equation, which assumes inviscid flow, is a reduced form of the Navier-Stokes equations and gives acceptable results.

The main objective of this study is to develop the interference between the two disciplines, namely structural dynamics and aerodynamics, in order to determine the dynamic aeroelastic properties of air vehicles. The present method is applied to solve the dynamic aeroelastic characteristics of the AGARD Wing 445.6. [15]

Method

For the dynamic aeroelastic analysis, a CFD solver, FLUENT, is coupled to governing equations of motion of the structure that are presented in the modal coordinates. The mode shapes and corresponding natural frequencies are obtained by using MSC/NASTRAN and used as an input for this approach. A FORTRAN code is developed in order to perform the entire computational procedure which is developed for the dynamic analysis. The flow chart of the iterative procedure is given in Fig.1.

In the developed coupling scheme, the dynamic aeroelastic simulation is started by computing an initial, steady-state solution for the undeformed wing which is used as the starting point of the unsteady dynamic

[1)] ROKETSAN Missile Industries Inc., P.K.: 30, 06780 Elmadağ-Ankara, TÜRKIYE

aeroelastic computations. At the start of the unsteady run, the pressure forces calculated at the wall-face centroids are splined to the structural grid nodes using the infinite spline method. The pressures calculated at the cell centers using FLUENT are used with the cell wall-face area vectors in order to calculate the pressure forces. Since the forces are at the cell centroids and not at the aerodynamic grid points, a spline matrix [S1] is created to spline forces between the wall-face centroids on the aerodynamic grid and the structural grid points using the transpose of the created spline matrix.

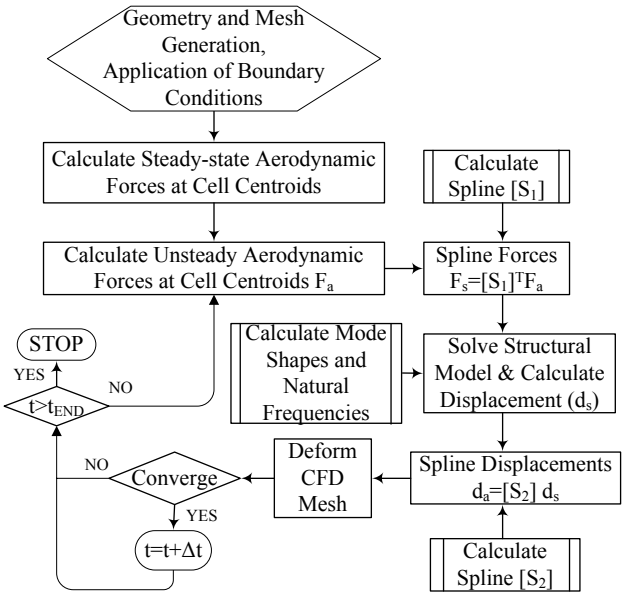

Figure 1. Flow Chart of the Dynamic Aeroelastic Procedure

The new deformed structural grid coordinates are then calculated in the modal coordinates using the linear modal structural model which is time marched using the Newmark method. In order to obtain the new coordinates of the aerodynamic grid, structural displacements are transformed to physical coordinates and splined using the second spline matrix [S2] between the structural grid points and the aerodynamic grid points. The computational fluid dynamic mesh is then deformed by using the FLUENT moving mesh algorithm. Finally, new flow variables are calculated for the next time-step. This process is repeated until a specified flow time is reached.

Since the AGARD Wing 445.6 has a symmetric NACA 65A004 airfoil, and the angle of attack is zero degree, an initial perturbation must be given in order to start the oscillations. One can use an initial force applied at some area of the wing, or can use an initial condition in the form of a velocity distribution. In the present study, the first mode shape of the structural model is used to create a sinusoidal velocity variation for one cycle with an amplitude of 0.5 m/s for the first mode frequency of the wing. Afterwards, unsteady coupled calculations are continued by removing the excitation and the wing is allowed to respond to unsteady aeroelastic loads.

The flutter points are calculated by using the aeroelastic model for different Mach numbers. At a selected dynamic pressure, the solution is computed for four cycles of the response. If the oscillations in the cycles are growing, a lower dynamic pressure value is chosen and the solution is recomputed. If the oscillations are convergent, higher dynamic pressure is chosen. This procedure is continued until the oscillations are neither decaying nor growing. Then, the dynamic pressure is determined which leads to neutral oscillations. This point of neutral oscillations is defined as the flutter point.

It may be possible to estimate the damping ratio, ζ, which yields a positive value for a stable solution, and a negative value for an unstable solution from a single response. For the dynamic aeroelastic calculations performed in this study, the structural damping was set to be zero, so the calculated damping ratio is purely of the aerodynamic origin. For a free-decaying, damped oscillation, the aerodynamic damping can be derived from the logarithmic decrement which is shown in eq.(1).

$$\zeta_n = \frac{1}{n}\ln\left(\frac{x_i}{x_{i+1}}\right) \tag{1}$$

where x_i and x_{i+n} are the peak amplitudes at a certain instant of time and taken after the n cycles of vibration, respectively.

Damping values are estimated for a large set of test points at constant Mach numbers for varying dynamic pressure values. The flutter boundary can then be determined by using linear interpolation in order to determine the dynamic pressure which yields the zero damping ratio. The accuracy of this method depends on the test points near to ζ=0; therefore, the flutter boundary estimation is improved by refining the study with more test points.

For the unsteady flow calculations, the pressure-velocity coupling algorithm, Pressure-Implicit with Splitting of Operators (PISO), is used with the second order upwinding scheme for density, momentum and energy equations. The MSC/NASTRAN finite element program is used to get the modal matrix and the corresponding natural frequencies, which are the main inputs of the coupling scheme.

The Flutter Speed Index (FSI) represents the condition where the magnitudes of the oscillations neither decrease nor increase, and is given by eq.(2):

$$V_f = \left(\frac{U_\infty}{b.\omega_\alpha\sqrt{\upsilon}}\right) \tag{2}$$

where b is the half chord length at the wing root, ω_α is the first torsion frequency and υ is the mass ratio described as eq.(3)

$$\upsilon = \left(\frac{\rho_{wing}V_{wing}}{\rho_{air}V_{cone}}\right) \tag{3}$$

where $V_{wing} = 0.0043584\ \mathrm{m}^3$ and $V_{cone} = 0.13054\,\mathrm{m}^3$, which is the volume of the truncated right cone enclosing wing.

Table 1. Experimental Flutter Data for the Weakened AGARD Wing 445.6

Mach	p_f [kg/m^3]	V_f [m/s]	FSI	ω/ω_α
0.499	0.42770	172.5	0.4459	0.5353
0.678	0.20818	231.4	0.4174	0.4722
0.960	0.06338	309.0	0.3076	0.3648
1.072	0.05512	344.7	0.3201	0.3617
1.141	0.07883	364.3	0.4031	0.4593

From the measured $\rho\infty$ and V_∞ values from the experiment [7], taking a gas constant of R = 287.05 Ks^2/m^2 and a specific heat constant of γ = 1.4 from gas dynamics and ideal gas assumption, one may obtain a temperature

value of T_∞ and a pressure value of P_∞. The experimental flutter data is shown in Table 1 for the AGARD Wing 445.6 at several points between Mach 0.499 and Mach 1.141.

Time Advancing Scheme

In the present study, a closely coupled approach is used for time advancing as illustrated in Fig.2. In this approach, corrective sub-iterations are performed at each time step until the fluid and the structure are synchronized and the entire aeroelastic system is fully converged. Then, new unsteady aerodynamic loads and corresponding structural displacements are calculated for the next time step. This process is repeated until a specified flow time is reached.

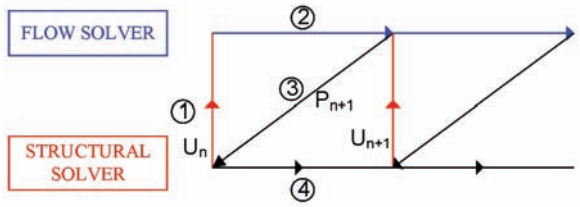

Figure 2. Closely Coupled Approach

In the closely coupled approach, fluid and structure systems are synchronized at each time step. A partitioned scheme is used for synchronization where fluid and structure solvers are separate. Fluid loads and structural displacements are exchanged within a single time step. The main advantages of the closely coupled approach are a synchronicity property and algorithmic flexibility for physically different systems [9].

Mesh Deformation

Mesh deformation in computational aeroelasticity applications is one of the important aspects and therefore it must be handled carefully. In order to represent the deformation of the structure during the aeroelastic simulation, the aerodynamic grid must be deformed consistently and the mesh quality must be maintained to avoid any numerical problem. Simply deforming the CFD grid is considerably cheaper and more convenient than the re-meshing of the entire CFD domain; therefore, it is commonly used in computational aeroelasticity.

FLUENT has the capability to interact with user-written programs, which allows a structural model to be coupled with it. FLUENT also has deforming mesh capabilities that can be controlled through a user-written subroutine referred to as a user-defined-function (UDF) in order to simulate the flow around a moving structure. In order to deform the CFD mesh using the results of the modal structural solution, the UDF code is developed.

In this study, the FLUENT moving mesh algorithm is used since the quality of the mesh can be easily controlled and preserved according to the pre-defined parameters. FLUENT consists of three mesh deformation methods which can be used to update the volume mesh in the deforming regions at the boundaries subject to the motion [2]. These methods are called spring-based smoothing, dynamic layering and local re-meshing.

In the spring-based smoothing method, the edges between any two mesh nodes are idealized as the interconnected springs which form a network. A displacement at a given boundary node will generate a force proportional to the displacement along all the springs connected to the node [2]. The spring-based method preserves mesh connectivity but needs a large amount of CPU time and memory. It is also limited to relatively small deformations when it is used as a standalone mesh deformation scheme. The second method, dynamic-layering, can be used in prismatic (hexahedral or wedge) mesh zones in order to add or remove layers of cells adjacent to a moving boundary, based on the height of the layer adjacent to the moving surface [2]. The third method is re-meshing. The cell quality may deteriorate and cells may degenerate if the boundary displacement is large compared to the local cell sizes. This leads to negative cell volumes which results in convergence problems in the flow solution. Re-meshing can eliminate the collapsed cells, but it adds extra computational costs. FLUENT replaces degenerated cells locally until new cells or faces satisfy the size and skewness criteria [2].

Interference between the Grids

Computational aeroelasticity requires a fluid-structure interface to transfer the aerodynamic loads and structural displacements at this common boundary, which is usually the wetted surface on the structure. The aerodynamic and structural grids generally do not coincide and do not lie on the same surface since the requirements are different for the corresponding systems. Therefore, the interpolation of aerodynamic pressure loads and displacements must be implemented between the two systems by a carefully implemented method. The performance of such a method depends on the accuracy and robustness of the interpolation scheme. Several studies in the literature raised the importance of the conservation of momentum and energy in the transfer of loads and displacements [9]. In order to transfer aerodynamic pressure loads from the CFD grid points to the CSD grid points, the transpose of the displacement transformation matrix, which ensures a conservative transfer of energy between the two systems, is used.

The prediction of complex dynamic aeroelastic phenomena such as flutter and limit cycle oscillations is sensitive to the conservation properties. An imbalance in the energy transfer between the fluid and structure systems causes instability and must be avoided [10].

The infinite plate spline method which is commonly used in aeroelasticity was firstly proposed by Harder and Desmarais [11]. This method is suitable for displacement and force transfer of wing-like components modeled by plate or shell elements. The infinite plane spline method solves the partial differential equation of equilibrium for an infinite plate with uniform thickness. Once the partial differential equation is solved, the deflection at other points, e.g. the aerodynamic points, on the plate can be determined [12].

Once the spline matrix is obtained, the displacements and the coordinates of the aerodynamic grid points can be computed from the displacements of the structural grid points with the following:

$$[\delta_a] = [S][\delta_s] \tag{4}$$

$$[q] = [q]_0 + [\delta] \tag{5}$$

where $[q]_0$ is the original undeformed grid. The grid coordinate matrices are defined as:

$$[q]=\begin{bmatrix} q_{x1} & q_{y1} \\ q_{x2} & q_{y2} \\ \vdots & \vdots \\ q_{xN} & q_{yN} \end{bmatrix} \tag{6}$$

The transformation of the forces from the aerodynamic grid to the structural grid can be performed by the transpose of $[S]$. Eq.(6) ensures the conservative transfer of energy between the flow and the structural systems [9].

$$[F_s]=[S]^T[F_a] \tag{7}$$

where the force matrix is defined as:

$$[F]=\begin{bmatrix} F_{x1} & F_{y1} \\ F_{x2} & F_{y2} \\ \vdots & \vdots \\ F_{xN} & F_{yN} \end{bmatrix} \tag{8}$$

The aerodynamic grid, used in the CFD calculations, is three-dimensional. In order to perform the infinite spline method, it is required that all structural grid points and aerodynamic grid points are located on the same plane. Therefore, the aerodynamic grid points are projected to the spline plane on which the structural grid points lie, in order to create the spline matrix. For the infinite spline method, two or more than two structural grid points cannot be located at the same x and y location. It is also important that for a given set of normal displacements at the structural grid points, the infinite spline method gives the displacements at the aerodynamic points only in the normal direction of the spline plane [12].

Structural Modal Approach

An aeroelastic simulation consisting of the non-linear CFD analysis coupled to a dynamic structural model is performed in order to investigate the structural deformation under an unsteady aerodynamic loading. This method allows a time-accurate non-linear analysis of dynamic behavior, leading to a much more accurate investigation of flutter [13]. The majority of such methods rely on the prediction of a structural response by the summation of a limited number of modes derived from the modal analysis using a commercial finite element solver.

The governing equation of motion of a structure can be written as:

$$[M]\frac{d^2w}{dt^2}+[C]\frac{dw}{dt}+[K]w=\{F(t)\} \tag{9}$$

$$w=\begin{pmatrix} w_1 \\ w_i \\ \vdots \\ w_N \end{pmatrix} \qquad F=\begin{pmatrix} F_1 \\ F_i \\ \vdots \\ F_N \end{pmatrix} \tag{10}$$

where N is the total number of the structural node. w_i and F_i are expressed as:

$$w_i=\begin{pmatrix} w_{ix} & w_{iy} & w_{iz} \end{pmatrix} \tag{11}$$

$$F_i=\begin{pmatrix} F_{ix} & F_{iy} & F_{iz} \end{pmatrix} \tag{12}$$

The displacement and force vectors at the node point i have three components in the 3-D space. Using the modal analysis, the dependent variables are expanded in terms of the natural free vibration modes as:

$$\{w(x,y,z,t)\}=\sum_{i=1}^{N} q_i(t)\{\varphi_i(x,y,z)\} \tag{13}$$

where $q_i(t)$ and $\{\varphi_i(x,y,z)\}$ are the generalized displacement vector and the mode shape matrix, respectively. The mode shape matrices are obtained by solving the eigenvalues of the free vibration problem. The modal decomposition of the structure motion is expressed as:

$$K\varphi=M\varphi\Lambda \tag{14}$$

or

$$K\varphi_j=\lambda_j M\varphi_j \tag{15}$$

A finite element structural solver may be used to solve eq.(15) and to obtain the mode shapes. The modal matrix and the eigenvalue matrix Λ is expressed as:

$$\varphi=[\varphi_1,...,\varphi_i,...,\varphi_{3N}] \tag{16}$$

$$\Lambda=diag[\lambda_1,...,\lambda_i,...,\lambda_{3N}] \tag{17}$$

The *j*-th eigenvalue can be defined by the natural frequency (ω) as:

$$\lambda_j=\omega_j^2 \tag{18}$$

The mode shape matrix is normalized with respect to the mass matrix and substituting eq.(18) into eq.(15)(and then multiplying by φ^T) yields:

$$\ddot{q}+[\xi]\dot{q}+[\omega]q=Q \tag{19}$$

where:

$$[\xi]=\varphi^T[C]\varphi \tag{20}$$

$$[\omega]=\varphi^T[K]\varphi \tag{21}$$

$$Q=\varphi^T[F] \tag{22}$$

the $[\omega]$ and $[\xi]$ matrices are diagonal and their terms are ω_i and $2\xi_i\omega_i$, respectively. Q is the generalized unsteady aerodynamic forces. The coupled system of equation can be rewritten as:

$$\ddot{q}_i+2\xi_i\omega_i\dot{q}_i+\omega_i q_i=Q_i, \quad i=1,2,...,N \tag{23}$$

where ξ_i and ω_i are the modal damping and the natural frequency for the ith mode, respectively. In this initial value problem, the Newmark algorithm [5] is used to solve eq.(23) for $q_{i,n+1}$ with the following set of equations, assuming a linear acceleration and no structural damping:

$$\begin{aligned} &\left(1+\frac{\Delta t^2}{6}\omega_i^2\right)\{\ddot{q}\}_{n+1}= \\ &=\{Q\}_{n+1}-\omega_i^2\left(\{q\}_n+\Delta t\{\dot{q}\}_n+\frac{\Delta t}{3}\{\ddot{q}\}_n\right) \end{aligned} \tag{24}$$

$$\{\dot{q}\}_{n+1} = \{\dot{q}\}_n + \frac{\Delta t}{2}\left(\{\ddot{q}\}_n + \{\ddot{q}\}_{n+1}\right) \quad (25)$$

$$\{q\}_{n+1} = \{q\}_n + \Delta t\{\dot{q}\}_n \frac{\Delta t^2}{6}\left(2\{\ddot{q}\}_n + \{\ddot{q}\}_{n+1}\right) \quad (26)$$

where n is the time step.

CFD Modeling and Simulation

The computational grids for the CFD simulations were generated by using GAMBIT commercial programs. The analyses were done with an unstructured commercial CFD solver FLUENT. The developed method is applied to solve the dynamic aeroelastic characteristics of the AGARD Wing 445.6, which is a well known test case for aeroelastic problems. Wind tunnel experiments have been conducted on the AGARD Wing 445.6 in the Langley Transonic Dynamics Tunnel in order to predict the dynamic response characteristics and the flutter boundary [7]. The AGARD 445.6 Wing has a taper ratio of 0.66, an aspect ratio of 1.65 and a wing swept of 45° at the quarter chord. It has the root and tip chords of 0.558m and 0.368m, and a semi span of 0.762m. The airfoil section in the stream--wise direction is a NACA 65A004 airfoil, which is a symmetric airfoil with a maximum thickness of 4 % of the local chord. The wing planform is shown in Fig.3.

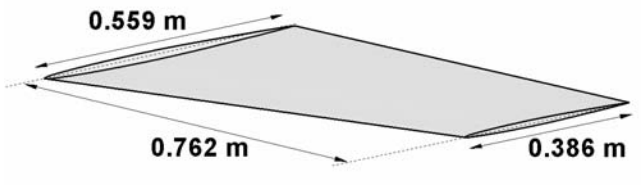

Figure 3. AGARD Wing 445.6 Planform

The dimensions of the computational domain and the defined boundary conditions for the AGARD Wing 445.6 are shown in Fig.4. The aerodynamic surface is defined as wall boundary conditions. The flow conditions such as Mach number, operating pressure, temperature and angle of attack are defined in the far-field boundary condition. In this study, the pressure-velocity coupling algorithm of PISO is applied with the second order upwinding scheme for density, momentum and energy equations.

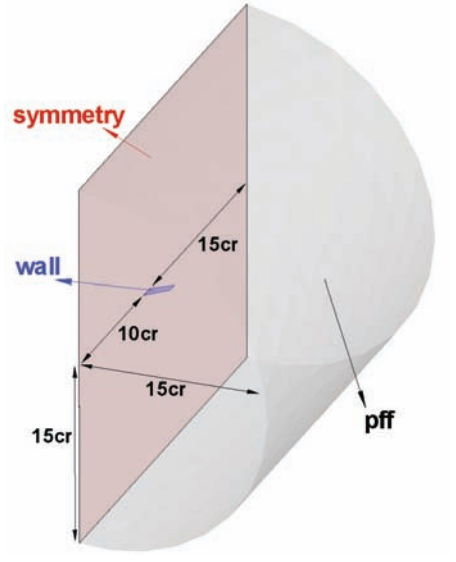

Figure 4. Dimensions of the CFD Domain

$$\frac{\partial}{\partial t}\int_V W dV + \oint [F]\cdot dA = \int_V H dV \quad (27)$$

where

$$W = \begin{Bmatrix} \rho \\ \rho u \\ \rho v \\ \rho w \\ \rho E \end{Bmatrix}, F = \begin{Bmatrix} \rho v \\ \rho v u + pi \\ \rho v v + pj \\ \rho v w + pk \\ \rho v E + pv \end{Bmatrix} \quad (28)$$

The pressure-based method linearizes the governing equations and solves the flow variables implicitly.

The optimum number of the surface triangular elements and the volume tetrahedral elements which are determined by the grid sensitivity analyses are shown in Table 2. The flow solution calculated with this grid is compared with the numerical results conducted by Cai [4], Lee and Batina [3].

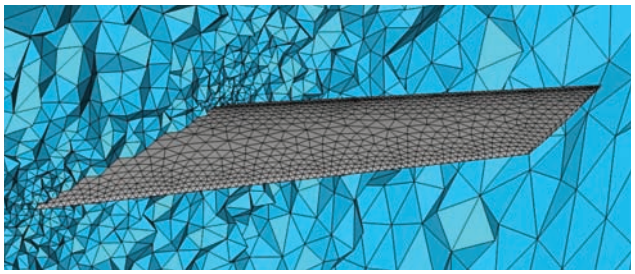

Figure 5. Computational Fluid Domain of the AGARD Wing 445.6

Table 2. Number of Surface Triangular and Volume Tetrahedral Elements

Number of Surface Triangular Elements	3,798
Number of Tetrahedral Elements	158,161

The pressure coefficient distribution over the AGARD Wing 445.6 is compared with the study of Cai [4]. Cai conducted a static aeroelastic analysis of the AGARD Wing 445.6 at the flow conditions M=0.85 and α=5°. The pressure coefficient distributions over the wing at % 34 span-wise locations for this flow condition are shown in Fig.7.

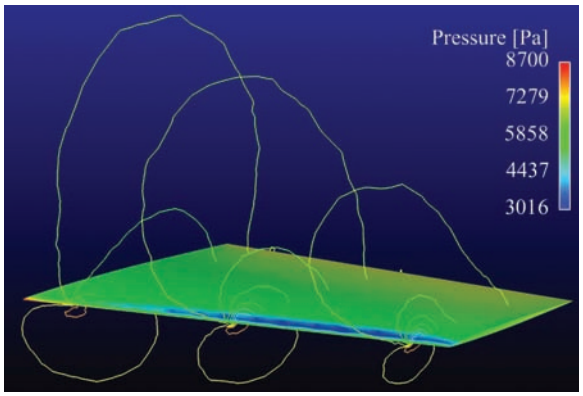

Figure 6. Pressure Contours over the AGARD Wing 445.6

The pressure coefficient distribution over the AGARD Wing 445.6 is compared with the study of Lee and Batina [3]. Lee and Batina conducted a dynamic aeroelastic analysis of the AGARD Wing 445.6 at the flow conditions M=1.141 and α=0°. The pressure coefficient distributions over the wing at 26% span-wise location are shown in Fig.8.

The results appear to agree well except for the leading edge. This difference may be attributed to the meshing technique. Cai [4] uses the O-Type structured grid, Lee and Batina [3] use the C-H type of grid which captures the leading edge radius accurately and gives a better resolution of the leading edge radius as compared to the present study.

In the present work, the unstructured grid and a limited number of triangular meshes are used [15].

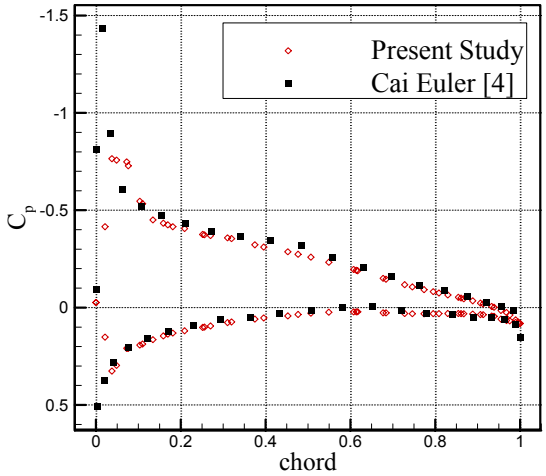

Figure 7. Comparison of Cp Distribution at %34 Semispan (M=0.85 α=5°)

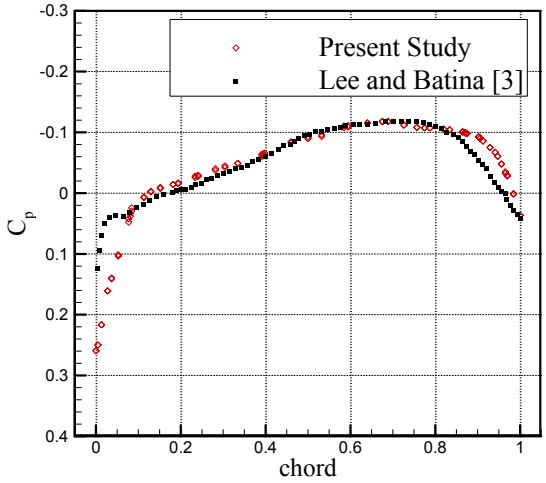

Figure 8. Comparison of Cp Distribution at %26 Semispan (M=1.141 α=0°)

CSD Modeling and Simulation

In this part, the details of the finite element analyses and the results of the modal analyses are given for the AGARD Wing 445.6. The finite element mesh for CSD analyses were generated by using the PATRAN commercial program. The analyses were done with a finite element structural solver, MSC/NASTRAN. The modal frequencies are compared with experimental data [7] in order to validate the structural finite element model used in the calculations in the following sections. In addition to the calculated modal frequencies, the mode shapes of the structure are also compared with the experimental study [7].

A weakened AGARD Wing 445.6 is modeled with the plate elements as a single layer orthotropic material the property of which is given in Table 3.

Table 3. Mechanical Properties for the Weakened AGARD Wing 445.6

Material Property	Value [Gpa]
E_1	3.1511 Gpa
E_2	0.4162 Gpa
G	0.4392 Gpa
ρ	381.98 kg/m^3
v	0.31

The rotations and translations of the nodes at the root section of the finite element model are fixed. Other nodes are allowed to translate in the out-of-plane direction. The CQUAD4 type of element is used for the finite element discretization. The grid sensitivity analysis for the structural grids is performed and the numbers of nodes for the span-wise and chord-wise directions for each finite element model are shown in Table 4.

Table 4. Number of Elements Used in the Finite Element Model

Number of Nodes for the Span-wise Direction	12
Number of Nodes for the Chord-wise Direction	12
Total number of Structured Element	121

The modal analysis of the weakened AGARD Wing 445.6 is performed using MSC/NASTRAN. The first four natural frequencies are given in Table 5 along with the experimental results [7] and those computed by Kolonay [8], Lee and Batina [3].

Table 5. Calculated Natural Frequencies for the Weakened AGARD Wing 445.6 [Hz]

	Mode 1	Mode 2	Mode 3	Mode 4
Present Study	9.41	39.46	48.96	94.35
Exp. (Yates) [7]	9.60	38.10	50.70	98.50
Kolonay [8]	9.63	37.12	50.50	89.94
Lee and Batina [3]	9.60	38.17	48.35	91.54

The mode shapes obtained from the finite element analysis of the weakened wing are scaled up so that the maximum and minimum values are the same as those in the experiments. The out-of-plane deflection contours are compared in Fig.10. It can be concluded that the results obtained from the finite element model appear to agree well with the experimental results.

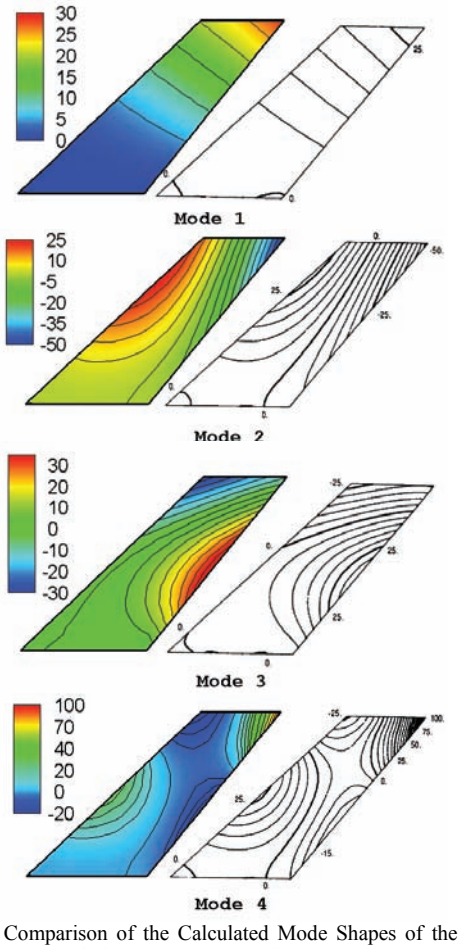

Figure 10. Comparison of the Calculated Mode Shapes of the AGARD Wing 445.6 (left) with the Experiments (right)

Time Interval Size

In order to determine the optimum time interval size, it is reduced until the aeroelastic simulation does not change by further decrease in the interval size. To achieve this, four different time interval sizes are examined. As it can be seen in Fig.9, the solution is affected by decreasing the time interval size up to the value of 0.001. A further decrease in the time interval size does not change the solution significantly. In this test case, the wing motion is mostly dominated by the first bending and the first torsion modes, which have natural frequencies of 9.6 Hz and 38.10 Hz, respectively [7]. The total time of a single period for these modes shall be 0.104 s and 0.025 s. These frequencies may change due to the unsteady aerodynamic forces. As the first estimate, choosing a time interval size of Δt = 0.001 will resolve these modes at 104 and 25 time steps, respectively. The time increment in the present study is the same in both aerodynamic and structural analyses.

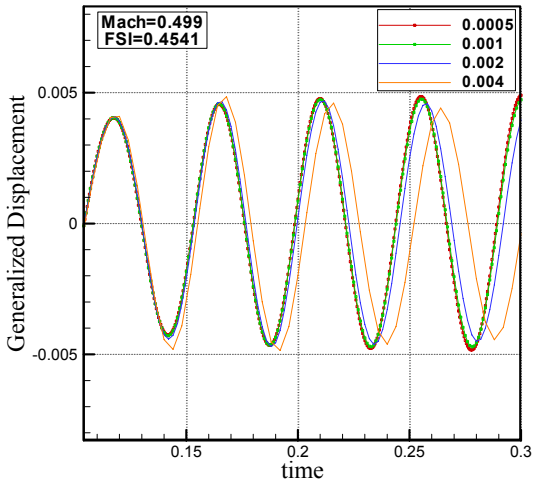

Figure 9. Examination of Time Interval Size

Results

The time histories of the first four generalized coordinates at FSI=0.4527, 0.4541, and 0.4557, M=0.499 are shown in Figs.11-13. The amplitude of the motion reduces at FSI=0.4527, when the flutter speed index is lower than the flutter critical speed. The amplitude of the motion is constant at FSI=0.4541, when the flutter speed index is equal to the flutter critical speed. The amplitude of the motion is growing at FSI=0.4557. It can be concluded that at M=0.499, the AGARD wing 445.6 has the flutter conditions with FSI=0.4541.

In order to determine the flutter boundary, damping estimations are collected for a large set of test points at M=0.499 for varying dynamic pressure values. For these test points, the estimated damping coefficients and the time histories of the first four generalized coordinates are given in Fig.14. The critical flutter speed can be determined from the flight conditions where damping coefficient is zero. At this Mach number, the static pressure is 36230.5 Pa, and the corresponding flutter speed is calculated as 171.84 m/s, which is very close to the experimental value of 172.46 m/s.

The results of the flutter analysis of the AGARD Wing 445.6 are compared with the experimental data and the results of the previous studies in Figs. 15-16 and 17, respectively. It can be concluded that the results of the flutter boundary and the flutter frequency of the AGARD Wing 445.6 for the Mach numbers ranging from 0.499 to 1.141 are in good agreement with the experimental results except for the region of the transonic dip where lower flutter speed is predicted. This can be attributed to the inviscid flow assumption. Including the viscous effects may improve the prediction of the FSI at this regime.

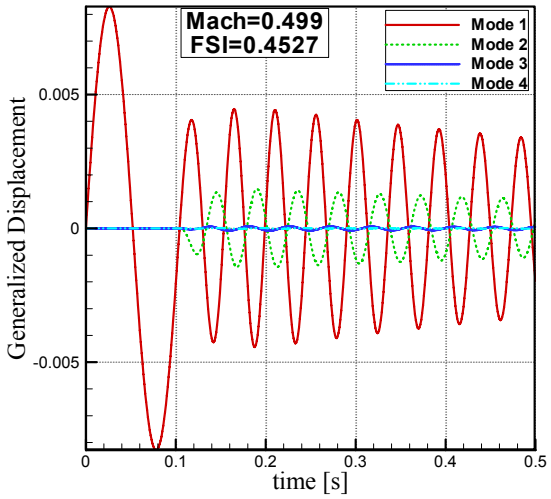

Figure 11. Time history of the first four generalized coordinates (M=0.499, FSI=0.4527)

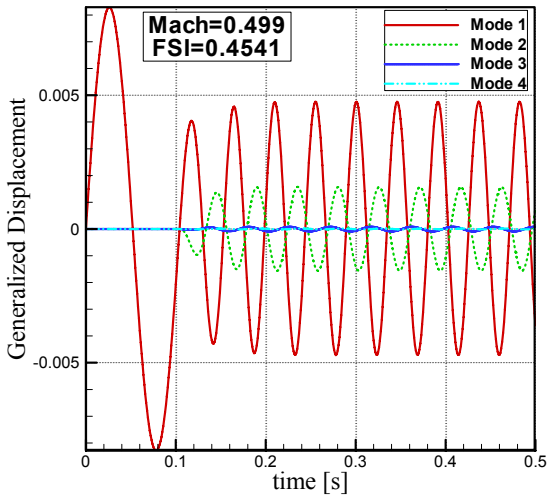

Figure 12. Time history of the first four generalized coordinates (M=0.499, FSI=0.4541)

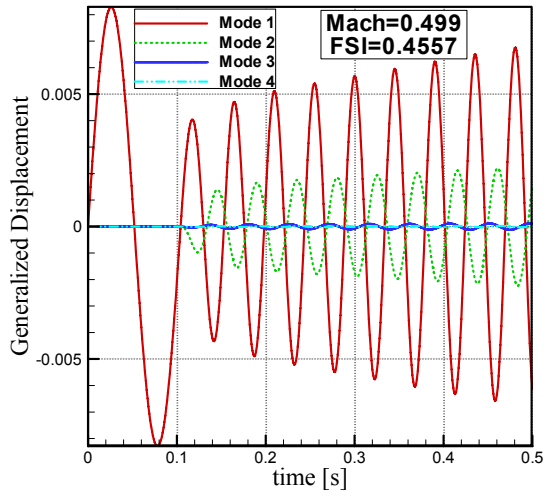

Figure 13. Time history of the first four generalized coordinates (M=0.499, FSI=0.4557)

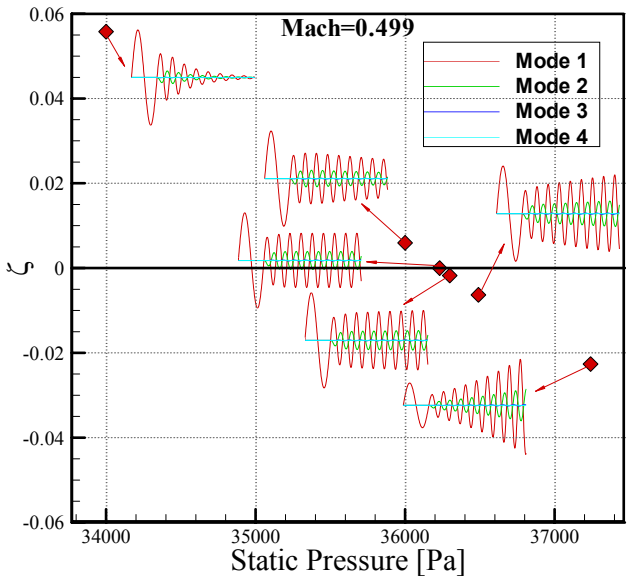

Figure 14. Flutter boundary test points, estimated damping coefficients and generalized displacements

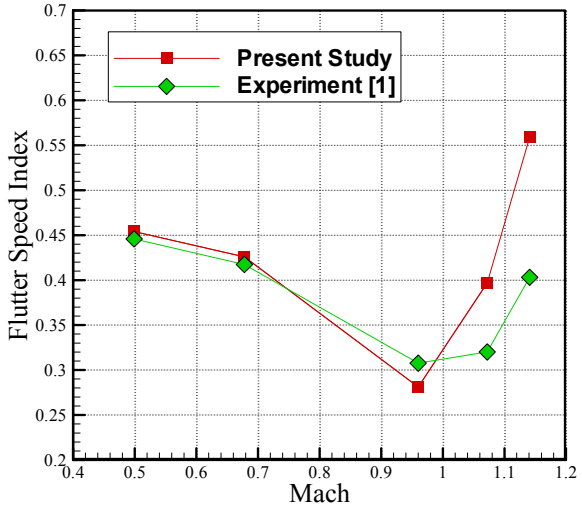

Figure 15. Comparison of the computed flutter speed index values and the experimental data

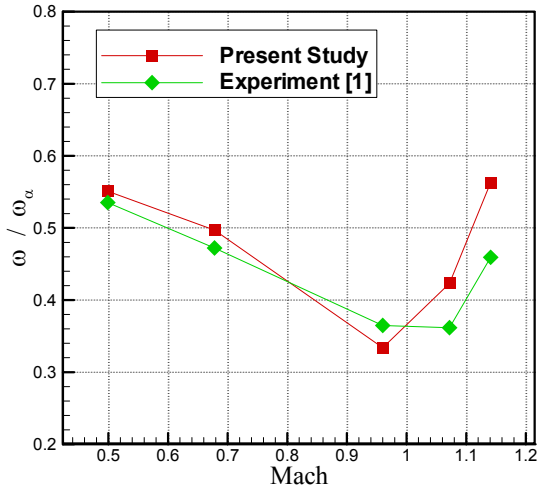

Figure 16. Comparison of the computed flutter frequency ratio with the experimental data of the AGARD wing 445.6

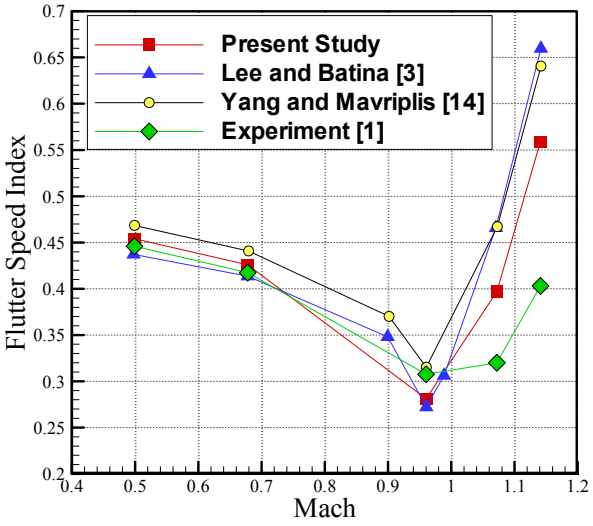

Figure 17. Comparison of the computed fsi values, the numerical data, and the experimental data of the AGARD wing 445.6

Conclusion

In this paper, a closely coupled approach is developed to solve the dynamic aeroelastic problems. A numerical method is developed to predict the aeroelastic response and the flutter boundary. The modal approach is used for a structural response and the Newmark algorithm is used for time marching. The mode shapes and corresponding natural frequencies are calculated by using MSC/NASTRAN. The unsteady flow field is solved by using a commercial CFD solver, FLUENT, in a parallel computing environment.

Mesh deformation techniques are investigated as a part of this research. In this study, the mesh deformation methods based on the FLUENT mesh deformation algorithm are used.

Predictions of complex dynamic aeroelastic phenomena such as flutter are sensitive to the energy conservation at the fluid-structure interface. An imbalance in energy transfer between the CFD and the CSD systems causes instabilities and an incorrect prediction of the aeroelastic behavior. Spline methods conserve the total force and moments on each system and are applicable to the dynamic aeroelastic problems.

The dynamic aeroelastic problem of the AGARD Wing 445.6 is solved with the developed procedure and the obtained results are compared with the numerical and experimental data available in the literature.

For the dynamic aeroelastic analysis, the FSI is determined for the AGARD Wing 445.6 at different Mach numbers ranging from 0.499 to 1.141. The flutter points are determined by running a solution for a significantly long period of time to arrive at a neutrally stable solution. Damping estimations are collected for a large set of test points at constant Mach numbers for varying dynamic pressure values. Then, the flutter boundary is determined yielding the zero damping ratio, ζ=0, where the amplitude of oscillations of the generalized displacement is neither decaying nor growing. The results of the present study are in good agreement with the experimental results except for the region of the transonic dip. Including the viscous effects may improve the prediction of the FSI at the region of the transonic dip.

References

[1] BAŞKUT,E.: *Development of a Closely Coupled Approach for Solution of Static and Dynamic Aeroelastic Problems*, METU, June, 2010.

[2] FLUENT 6.3 Documentation. FLUENT, Inc., 2006.

[3] Lee-Rausch,M.E., Batina,T.J.: *Calculation of AGARD Wing 445.6 Flutter Using Navier-Stokes Aerodynamics*, AIAA 93-3476.

[4] CAI,J., LIU,F., TSAI,H.M., WONG,A.S.F.: *Static Aero-elastic Computation with a Coupled CFD and CSD Method*, AIAA 2001-0717, Aerospace Sciences Meeting and Exhibit, 39th, Reno, NV, Jan. 8-11, 2001.

[5] PARKER,G.H.: *Dynamic Aeroelastic Analysis of Wing/Strore Configurations*, Air Force Institute of Technology Air University December 2005.

[6] WRIGHT,J.R., COOPER,J.E.: *Introduction to Aircraft Aeroelasticity and Loads*, John Wiley & Sons Inc., 2007.

[7] YATES,E.C.: *AGARD Standard Aeroelastic Configurations for Dynamic Response I-Wing 445.6*, AGARD Report 765, North Atlantic Treaty Organization, Group for Aerospace Research and Development, 1988.

[8] KOLONAY,R.M.: *Unsteady Aeroelastic Optimization in the Transonic Regime*, Ph. D. Thesis, Purdue University, 1996.

[9] MATHEW,F.B., JEFFREY,L.P.: *Methods for Simulation-based Analysis of Fluid-Structure Interaction*, Sandia National laboratories, 2005.

[10] MURAYAMA,M., NAKAHASHI,K., Matsushima,K.: *Unstructured Dynamic Mesh for Large Movement and Deformation*, AIAA 2002-0122, 2002.

[11] HARDER,R.L., DESMARAIS,R.N.: *Interpolation Using Surface Splines*, AIAA Journal, 1972, Vol.9, No.2, pp.189-191.

[12] "*ZAERO version 8.3 Theoretical Manual*". ZONA Technology, Inc., Scottsdale, AZ, 19 edition, 2008

[13] TAYLOR,N.V., ALLEN,C.B.: *Investigation of Structural Modelling Methods for Aeroelastic Calculations* AIAA 2004-5370 22nd Applied Aerodynamics Conference and Exhibit, Rhode Island, 2004.

[14] YANG,Z., MAVRIPLIS,D.J.: *Higher-order Time Integration Schemes for Aeroelastic Applications on Unstructured Meshes*, American Institute of Aeronautics and Astronautics.

[15] BAŞKUT,E., AKGÜL,A.: *Development of a Coupling Procedure for Static Aeroelastic Analyses*, Sceantific Technical Review, ISSN 1820-0206, 2011, Vol.61, No.3-4, pp.39-48.

Received: 16.01.2012.

Razvoj spregnute procedure za dinamičku aeroelastičnu analizu

U radu je je razvijen numerički metod za analizu aeroelastičnog odgovora i flatera elastičnih struktura. Spregnuti pristup je korišćen za vremensku analizu. Solver za opisivanje strujanja bazira na Ojlerovim jednačinama sa diskretizacijom primenom konačnih zapremina. Modalna analiza je korišćena sa strukturalni odgovor u sprezi sa Newmark-ovim algoritmom za vremenski odgovor. Da bi smo menjali podatke pomeranja i pritiska između strukturne i aerodinamičke mreže korišćen je beskonačni metod splajna. Mreža CFD je pomerana na principu opruge i metodi lokalne reformulacije mreže kakva je korisniku na raspolaganju u okviru softverskog paketa FLUENT da bi adaptirao novi oblik aerodinamičke površine u svakoj aeroelastičnoj iteraciji. Krilo tipa AGARD 445.6 je modelirano i rešeno sa razvijenom procedurom a dobijeni rezultati su upoređeni sa raspoloživim numeričkim i eksperimentalnim rezultatima iz literature.

Ključne reči: **aeroelastičnost, dinamička aeroelastičnost, krilo, flater, metoda konačnih razlika, algoritam.**

Порядок разработки связанной методики для динамического аэроупругого анализа

В настоящей работе разработан численный метод для анализа аэпоупругого ответа и трепета упругих конструкций. Связанный подход использован для временного анализа. Решатель для описания потока основывается на уравнениях Эйлера с конечным объёмом дискретизации. Модальный анализ был использован со структурными ответами в сочетании с алгоритмом Ньюмарка для временного отклика. Для того чтобы изменить данные движения и давления между структурными и аэродинамическими сетками используется бесконечный метод сплайн. Сеть CFD перемещается принципом пружины и метода местных источников и переработки в сторону такой сети доступной пользователю в пакете программного обеспечения FLUENT, адаптированного к новой форме аэродинамических поверхностей на каждой аэроупругой итерации. Крыло типа AGARD 445.6 смоделировано и решено с разработанной методикой и полученные результаты были сопоставлены с имеющимися расчётными и экспериментальными результатами из литературы.

Ключевые слова: **аэроупругость, динамическая аэроупругость, трепетание крыльев, метод конечных разниц, алгоритм.**

Développement de la procédure couplée pour l'analyse dynamique de l'élasticité aérienne

Dans ce papier on a développé une méthode numérique pour l'analyse de la réponse élastique aérienne et des battements des structures élastiques. L'approche couplée a été utilisée pour l'analyse temporelle. Le solveur pour la description des courants est basé sur les équations de Euler avec la discrétisation par l'emploi des volumes finies. L'analyse modale a été utilisée pour la réponse structurale couplée avec l'algorithme de Newmark pour la réponse temporelle. Dans le but de changer les données de déplacement et de la pression entre le réseau structurale et celui aérodynamique on a utilisé la méthode infinie spline. Le réseau CFD a été déplacé sur le principe du ressort et de la méthode de formulation locale du réseau dont l'utilisateur dispose dans le cadre du progiciel FLUENT pour adapter une nouvelle forme de la surface aérodynamique dans chaque itération aérienne élastique. L'aile AGARD 445.6 a été modelée et résolue par la procédure développée et les résultats obtenus ont été comparés avec les résultats numériques et expérimentaux disponibles dans la littérature.

Mots clés: **élasticité aérienne, élasticité aérienne dynamique,aile, battement, méthode des différences finies, algorithme.**